

Optimal design of illuminant for improving intraoperative color appearance of organs

Abstract: When surgeons evaluate the condition of organs and make diagnoses, color difference is important information despite its subtleness. Yielding clearer views of blood circulation holds the key to successful surgeries such as transplants and anastomosis. Optimization of surgical illuminant is one approach to clearer views. Our previous study focused on computer simulation to enhance color difference. In the present study, we improved the simulation method by applying a color appearance model CIECAM02 and we realized an optimized illuminant based on the simulation. In an evaluation experiment comparing the optimal illuminant with the conventional illuminant, fourteen LEDs fixed to the light unit were spectrally adjusted to demonstrate the two illuminants. Using a rat cecum, we observed the color differences under two conditions: normal blood flow and restricted blood flow. The color difference under the optimal illuminant was greater than under the conventional illuminant and the effectiveness of the optimal illuminant was confirmed.

Keywords Surgical illumination · Spectrally tunable light source · Color difference enhancement · Intraoperative color appearance

1 INTRODUCTION

In open surgery, visual diagnosis plays an important role in realizing a successful surgery when identifying conditions of organs and recognizing target sites. For example, in autotransplantation, a healthy part of the digestive tube of a patient is resected and used to construct a diseased part. In this operation, it is very important to judge if the healthy part to be transplanted is viable and compatible with other organs. The organ color is one of the most important pieces of information for this judgement. However, the color difference to distinguish between health and disease is often subtle, and surgeons largely depend on their experience and sense when judging condition.

To mitigate the problem of color difference, the use of some imaging devices such as multispectral cameras has been proposed [1-3]. This proposal assumes that surgeons capture multispectral images of organs of interest with a color-rich camera and check the enhanced or transformed images to identify the condition. In the case of laparoscopic surgery, such devices might be effective because such surgery premises the use of an imaging device and display device. However, application of these devices in open surgery might hinder the smooth workflow because of their bulky setup and the complicated procedure to reach the judgement.

When open surgery is performed under a surgeon's direct observation of the surgical region, spectral characteristics of the illuminant are the most important factor for the organ color judgement. Namely, optimization of illuminant may lead to better diagnosis by the surgeon. Some previous studies used computer simulations to optimize the illuminant [4-6]. In [7] and [8] the authors optimized the light-emitting diode (LED) light spectrum for surgical lighting and

implemented a LED ceiling system. They optimized the spectrum so as to maximize the gray-level contrast.

We have also been developing an LED-based lighting system designed for surgery [9]. While the authors in [7] and [8] maximized the gray-level contrast, we aimed at maximizing the specific color difference between healthy and ischemic statuses (our first constraint). Another novelty we have considered is the introduction of an additional constraint related to the whiteness of illuminant. Surgeons are used to the conventional shadow-less white light in an operation room. Thus, an extreme change in color of the organ will confuse surgeons even if it enhances the color difference between the two statuses. The second constraint was introduced to avoid such an extreme change. Hence, in optimization of illuminant, our two constraints were the color difference between healthy and ischemic statuses and the whiteness of the illuminant. These two constraints were defined to obtain illuminant which enables enhancement of color differences and is close to the conventional shadow-less white light at the same time.

In [9], we used the color space CIELAB for calculating color difference and only presented the computer simulation results. In this paper, we used a more advanced color appearance model CIECAM02 in the optimization. We also prototyped a spectrally tunable light source with LEDs and implemented an optimized illuminant obtained by the simulation. In this setup, the light source consists of 14 kinds of commercially available LEDs with different spectral distributions. By controlling the intensity of each LED distribution, we also demonstrated a conventional shadow-less white light for comparison. Using the prototype tunable light source, we conducted an *in vivo* experiment with rat cecum and evaluated the effectiveness of the optimal illuminant.

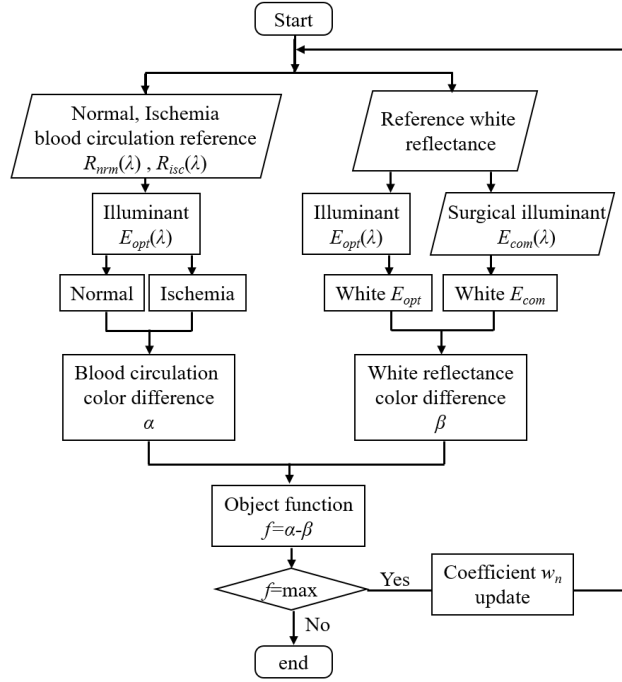


Fig. 1 Flow chart of illumination optimization

2 Method of spectral distribution optimization

In this section, we formulate an objective function used in the optimization. An optimal illuminant $E_{opt}(\lambda)$ is given by a combination of spectral radiations of LEDs and is expressed by Eq. (1):

$$E_{opt}(\lambda) = \sum_{n=1}^N w_n E_n(\lambda) \quad (1)$$

$$0 \leq w_n \leq 1, n=1, \dots, N.$$

Here N is the number of LEDs and $E_n(\lambda)$, $n=1, \dots, N$ denotes the normalized spectral radiation of each LED. w_n denotes the weight for the n -th LED and it ranges from 0 to 1. In the optimization, the weights $\{w_n\}$ are the parameters to be optimized.

Letting the spectral reflectance of a reflective object be $R(\lambda)$, the spectral energy from the reflected light is given by $E_{opt}(\lambda)R(\lambda)$. The color perceived by the standard human observer is modeled by tri-stimulus values, X , Y , Z , and is given by

$$\begin{aligned} X &= k \int \bar{x}(\lambda) E_{op}(\lambda) R(\lambda) d\lambda \\ Y &= k \int \bar{y}(\lambda) E_{op}(\lambda) R(\lambda) d\lambda \\ Z &= k \int \bar{z}(\lambda) E_{op}(\lambda) R(\lambda) d\lambda. \end{aligned} \quad (2)$$

Here, $\bar{x}(\lambda)$, $\bar{y}(\lambda)$, $\bar{z}(\lambda)$ are the color matching functions which are related to the spectral sensitivity of cones in the retina, defined by the International Commission on Illumination (CIE). The constant value k is defined as 100 divided by the value Y . When the color difference is evaluated, a uniform color space, CIELAB is often used. The values L^* , a^* , b^* in CIELAB color space are calculated from XYZ values. We used the CIELAB color space for the evaluation of color difference in our previous paper [9]. In this paper, we use a more advanced color appearance model in the optimization of illumination. This model was defined in 2002, and is known as CIECAM02 [10]. Namely, we calculate color difference $\Delta E'$ defined in CIECAM02 from XYZ tri-stimulus values taking account of the surroundings such as the illumination conditions. Details of CIECAM02 are described in the appendix.

We define the optimal illuminant as a white illuminant which can enhance the color difference between healthy and ischemic statuses. In this paper, we called the data collected under normal blood flow as “Normal”, and the data collected under restricted blood flow as “Ischemia”. The spectral reflectance of a “Normal” and “Ischemia” is represented by $R_{nrm}(\lambda)$ and $R_{isc}(\lambda)$, respectively. In this method, we use two kinds of color differences, $\alpha(E_{opt}(\lambda))$ and $\beta(E_{opt}(\lambda))$. $\alpha(E_{opt}(\lambda))$ expresses color the difference between “Normal” and “Ischemia” under the spectral distribution $E_{opt}(\lambda)$, and $\beta(E_{opt}(\lambda))$ expresses the color difference of a perfect diffuser (white object) under two illuminants, the optimal

illuminant and the conventional illuminant. For our purpose as mentioned above, it is desirable that $\alpha(E_{opt}(\lambda))$ is large and $\beta(E_{opt}(\lambda))$ is small. Thus, we define the objective function in the optimization as

$$f(E_{opt}(\lambda)) = \alpha(E_{opt}(\lambda)) - \gamma \cdot \beta(E_{opt}(\lambda)) \quad (3)$$

and find a solution $E_{opt}(\lambda)$, or more explicitly speaking, the set of weights $\{w_n\}$ that maximizes $f(E_{opt}(\lambda))$. The balance between two terms, $\alpha(E_{opt}(\lambda))$ and $\beta(E_{opt}(\lambda))$, can be adjusted by the whiteness parameter γ which can change the similarity of white object under two illuminants. The larger the value γ is, the more similar the color of the white object under the two illuminants is. Figure 1 shows the flow of the illumination optimization. Particle swarm optimization is used as an optimization method [11].

3. Experiment

3.1 Optimal design of illuminant spectra

3.1.1 Data collection of blood circulation condition for illuminant design

A rat was used in this experiment for the proof of concept because obtaining promising results in preclinical tests are required before clinical application. We captured images of the cecum of a rat with a hyper spectral camera and calculated spectral reflectance. The camera was NH-8 (EBA JAPAN Co.) which has 1200×1024 pixels, 12 bits per pixel and covers the spectral range from 380 to 1000 nm with 5 nm intervals. Lighting and imaging geometry were based on the CIE recommendation [12]. Namely, a xenon light was illuminated normal to the target and the image was captured from the 45-degree direction. After the abdomen of the rat under anesthesia was opened, the cecum was pulled out and fixed on a jig with its blood circulation maintained. As a reference, a perfect diffuse reflector was put near the target so that it was captured with the target cecum in the same image and used for calculation of reflectance of the target cecum.

The observation was performed under the two conditions. In the first step, the hyperspectral image of a certain region of the rat cecum under normal blood circulation was captured, which we refer to as “Normal” in this paper. Next, the images of the same area of the rat cecum were captured for 3 minutes after blocking blood circulation. The data obtained under this condition were defined as “Ischemia”. We calculated an average spectral reflectance of the rat cecum region from captured hyperspectral images. Figure 2 shows the spectral

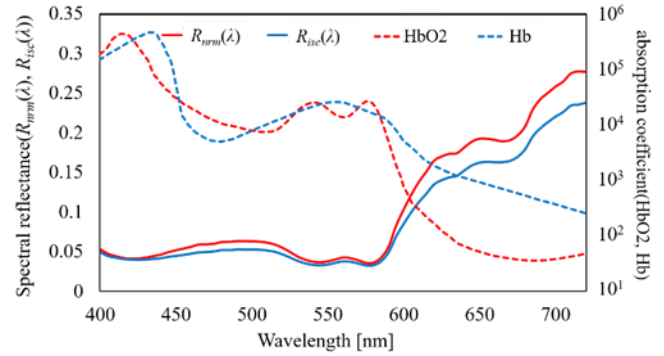


Fig. 2 Spectral reflectance of blood circulation (solid lines) and spectral absorption of Hb and HbO₂ (dashed lines)

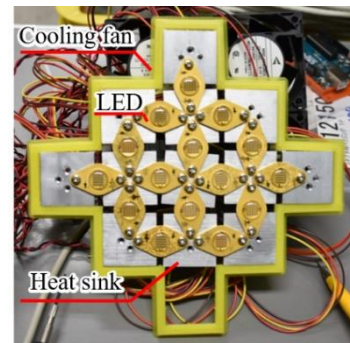
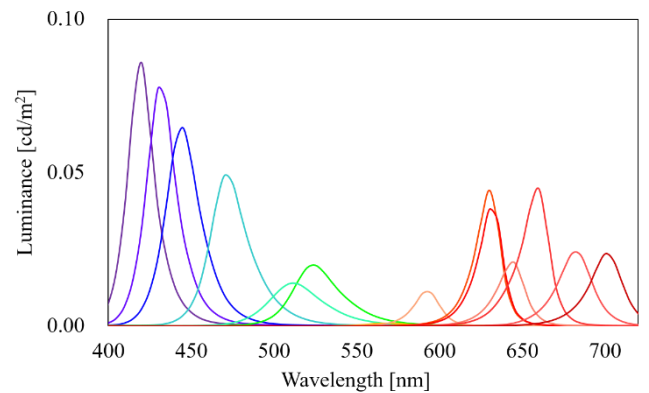
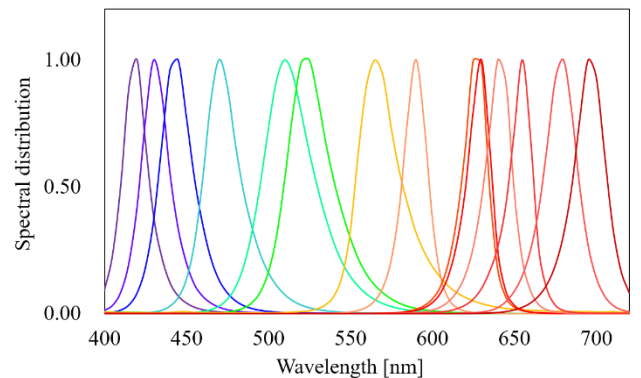


Fig. 3 LEDs mounted on the light source unit



(a) Measured spectra of each LEDs



(b) Normalized spectra of LEDs

Fig. 4 Spectral distributions of LEDs

reflectance results for “Normal” $R_{nm}(\lambda)$ and “Ischemia” $R_{isc}(\lambda)$ cases. Two spectral reflectances showed remarkable differences especially in the long wavelength region. These differences could probably be caused by absorption and scattering of hemoglobin, HbO_2 , and deoxygenated hemoglobin, Hb . The proportion of Hb to HbO_2 increased as a result of blocking the blood flow. Hb has a higher absorption coefficient in the wavelength ranging from 600 to 720 nm compared with HbO_2 . Therefore, the difference of spectral reflectance between the healthy and ischemic statuses was affected by absorption coefficients of Hb and HbO_2 .

3.1.2 Prototyping a spectrally tunable light source with LEDs

We prototyped a spectrally tunable light source with 14 commercially available LEDs (Ushio Epitex Inc.). Figure 3 shows a photo of the LEDs mounted on the light source unit. High intensity LEDs were used so as to produce enough illuminance. Fourteen bands of LEDs were chosen to cover the visible range as uniformly as possible. The peak wavelengths were 420, 430, 450, 470, 505, 525, 565, 590, 620, 630, 645, 660, 680, 700 and 720 nm. Although the spectral characteristics of each LED are disclosed by the manufacturer in a general data sheet, we measured them using a spectral radiance meter, SR-LEDW (Topcon Co.) to obtain individual exact characteristics. Figure 4a shows the measured spectra of each LED under the same electric current and Fig. 4b shows the intensity normalized by each peak intensity, $E_n(\lambda)$, $n=1, \dots, 14$. The optimum weights $\{w_n\}$ were first corrected to compensate for the intensity variation between LEDs and then controlled by the pulse-width modulation to achieve the intended balance.

3.1.3 Designed illuminant and prediction of color enhancement

We calculated the optimal illuminant that maximizes the objective function of Eq. (3) for three values of γ , *i.e.*, 0.5, 1.0 and 1.5. Figure 5 shows the calculated spectral distribution. In all cases, the largest spectrum peak was around 620 nm, and the second largest was around 505 nm. These two peaks were located in areas which showed remarkable difference between spectral reflectance of healthy and ischemic statuses. While the illuminants for $\gamma = 0.5$ and 1.0 were similar, the illuminant for $\gamma = 1.5$ had another peak around 420 nm and had a broader shape than the others. This broad shape was thought to keep whiteness. We then predicted the color difference of the two statuses

under the optimum illuminant. For comparison, the color difference under a conventional shadow-less white was also calculated. Table 1 shows predicted color differences between “Normal” and “Ischemia” under the two illuminants. The larger the γ value was, the smaller the color differences between the optimal illuminants and the conventional illuminant and the smaller the color differences between “Normal” and “Ischemia”.

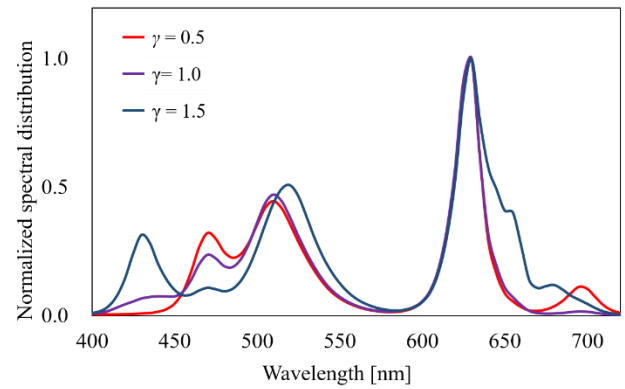


Fig. 5 The optimal illuminant

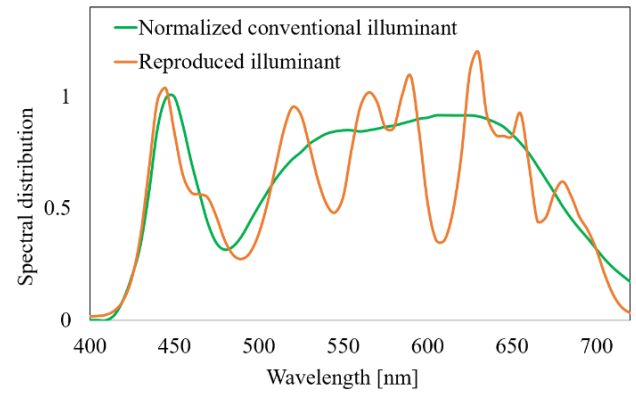


Fig. 6 The conventional illuminant



Fig. 7 Setup for the evaluation experiment

Table 1: Color difference in simulation

	Conventional illuminant	Optimal illuminant		
	(Skylux Crystal)	$\gamma = 0.5$	$\gamma = 1.0$	$\gamma = 1.5$
Color difference $\Delta E', \alpha$ (Normal-Ischemia)	1.54	2.84	2.76	2.24
Color difference $\Delta E', \beta$ (Whiteness)	0.0	0.70	0.45	0.21

3.2 Evaluation experiment

We then reproduced the spectral distribution of the optimal illuminant for $\gamma = 1.0$ with the spectrally tunable light source. For the purpose of comparison, the conventional illuminant, Skylux Crystal, was also reproduced with the same light source. The intensities of LEDs were set by the least squares method. Figure 6 shows the conventional illuminant spectrum and its approximated spectrum. Figure 7 shows the setup for the evaluation experiment.

Figure 8 shows color differences of the target cecum before and after blocking the blood flow. For reference, predicted colors of the region of interest before and after blocking the blood flow are also shown. However, it should be noted the reproduction is not exact because the resulting color printed on this paper is beyond our control. This table Shows that the color difference between “Normal” and “Ischemia” under the optimal illuminant was larger than that under the conventional illuminant in all cases. These values

were larger than the simulated values shown in Table 1. We could attribute it to a probable difference in the blood blocking conditions.

4 Discussion and conclusion

This paper proposed the optimization method of surgical illuminant aiming at enhancing the color difference of blood circulation. Changes in Hb and HbO₂ concentration are considered to be a contributing factor to color transition, which is considered to be universal in human beings and animals. Therefore, we conducted a baseline study using a rat cecum by blocking blood flow. The experiment was performed to obtain to types of data: “Normal” and “Ischemia”.

The optimal illuminant, shown in Fig 5, had a bimodal spectral distribution whose peaks were around 505 nm and 620 nm. We presumed color differences in these peaks coincided with those of spectral reflectance shown in Fig. 2. We confirmed that whiteness level of illuminant can be































Color difference $\Delta E'$		Elapsed time[min]				
		4	8	12	16	20
Sample 1	Conventional illuminant	 3.93	 4.00	 3.88	 4.06	 3.42
	Optimal illuminant	 4.44	 4.12	 3.95	 4.75	 3.87
Sample 2	Conventional illuminant	 3.73	 4.07	 4.43	 4.97	 4.32
	Optimal illuminant	 6.15	 6.16	 5.96	 7.15	 8.88
Sample 3	Conventional illuminant	 8.67	 8.29	 8.90	 8.71	 10.28
	Optimal illuminant	 10.20	 9.62	 11.28	 9.63	 10.26

Fig. 8 Color samples and color differences $\Delta E'$ under the conventional and the optimal illuminants

operated by controlling whiteness parameter γ . The whiteness of the illuminant was incompatible with enhancement in color difference of blood circulation.

To confirm the effectiveness of the simulation, we prototyped the spectrally tunable light source so as to evaluate the effectiveness of the optimal illuminant. The light quantity of the spectrally tunable light source was sufficient for the evaluation experiment because the size of the target region was small. Broad angle diffusion of LEDs which were mounted on the spectrally tunable light source provided uniformity of illumination.

Figure 8 shows results indicating color differences $\Delta E'$ based on CIECAM02 under the optimal illuminant were greater than under the conventional one in almost all the measured data, which suggests that the optimal illuminant was superior to the conventional one. However, in some cases, the color of the tissue changed greatly as a result of enhancement process because we did not put great importance on average tissue color.

To prevent extreme change in the tissue color and to enhance color difference at the same time, another simulation method using average tissue color spectra instead of a perfect diffuser (white object) and calculation of $\beta(E_{opt}(\lambda))$ would be promising. We tested this approach and confirmed that color difference between healthy and ischemic statuses were enhanced while retaining the operation field color. However, the enhancement we obtained through the simulation was limited. For our future research, further evaluation experiment and investigation on subjective evaluation by direct observation with the help of clinicians would be required.

ACKNOWLEDGEMENT

This research was partly supported by KAKENHI, the Grant-in-Aid for Scientific Research (A), Grant Number 16H01855, and JSPS Core-to-Core Program A. Advanced Research Networks.

REFERENCES

- [1] Akbari H (2010) Detection and analysis of the intestinal ischemia using visible and invisible hyperspectral imaging. *IEEE Trans Bio Eng* 57(8):2011-2017
- [2] Zuzak KJ, Francis RP, Wehner EF, Litorja M, Cadeddu JA, Livingston E H (2011) Active DLP hyperspectral illumination: a noninvasive, in vivo, system characterization visualizing tissue oxygenation at near video rates. *Ana Chem* 83(19):7424-7430
- [3] Bartczak P, Fält P, Penttinen N, Ylitepsa P,

Laaksonen L, Lensu L, Hauta-Kasari M, Uusitalo H (2017) Spectrally optimal illuminations for diabetic retinopathy detection in retinal imaging. *Opt Rev* 24(2):105-116

- [4] Wang, H, Yung-Tsan C (2012) Optimal lighting of RGB LEDs for oral cavity detection. *Opt Express* 20(9):10186-10199.
- [5] Litorja M, Brown SW, Lin C, Ohno Y (2009) Illuminants as visualization tool for clinical diagnostics and surgery. *Proc. SPIE 7169*, National Institute of Standards and Technology, CA, USA
- [6] Wang HC, Tsai MT, Chiang, CP (2013) Visual perception enhancement for detection of cancerous oral tissue by multi-spectral imaging. *J. Opt* 15(5):055301.
- [7] Liu, P, Wang, H, Zhang, Y, Shen, J, Wu, R, Zheng, Z, Li, H, Liu, X (2014) Investigation of self-adaptive LED surgical lighting based on entropy contrast enhancing method. *Opt Comm* 319:133-140.
- [8] Shen, J, Wang, H, Wu, Y, Li, A, Chen, C, Zheng, Z (2015) Surgical lighting with contrast enhancement based on spectral reflectance comparison and entropy analysis. *J. Biomed. Opt* 20(10):105012
- [9] Murai, K, Kawahira, H, Haneishi, H (2013) Improving color appearance of organ in surgery by optimally designed LED illuminant, *World Cong on Med Phys and Biomed Eng*, 1010-1013.
- [10] Luo, MR, Li, C (2013) CIECAM02 and its recent developments. In: *Advanced Color Image Processing and Analysis*. Springer, New York, Wiley. pp. 19-58.
- [11] Kennedy, J (2011) Particle swarm optimization. In: *Encyclopedia of Machine Learning*, Springer. pp. 760-766.
- [12] Wyszecki G, Stiles, WS (1982) *Color Science*, 2nd ed., John Wiley & Sons. New York, Wiley.

APPENDIX Formula of CIECAM02

As a first step to calculate color difference, tri-stimulus values were modified to the CAT 02 space, R, G, B , which is one of the color uniformity spaces, and written as follows,

$$\begin{bmatrix} R \\ G \\ B \end{bmatrix} = \mathbf{M}_{\text{CAT02}} \begin{bmatrix} X \\ Y \\ Z \end{bmatrix} \quad (\text{A1})$$

$$\mathbf{M}_{\text{CAT02}} = \begin{bmatrix} 0.733 & 0.430 & -0.162 \\ -0.704 & 1.698 & 0.0061 \\ 0.003 & 0.0136 & 0.983 \end{bmatrix}.$$

The D factor for adaption degree is defined as follows,

$$D = F \left[1 - \frac{1}{3.6} e^{\left(\frac{-(L_A+42)}{92} \right)} \right]. \quad (\text{A2})$$

The adaption luminance L_A is defined as illumination luminance divided by 5π . In this paper, we set $L_A = 20,000$ lx and $F = 1$. Then D is given by 0.87. Using the CAT02 uniform space value and the D factor, we define the full chromatic adaption transform as follows,

$$\begin{aligned} R_C &= [(Y_W \cdot D / R_W) + (1 - D)]R \\ G_C &= [(Y_W \cdot D / G_W) + (1 - D)]G \\ B_C &= [(Y_W \cdot D / B_W) + (1 - D)]B. \end{aligned} \quad (A3)$$

Here, R_W , G_W , B_W are CAT02 values of illumination. The full chromatic adaption values are converted to the Hunt- Pointer Estevez space before the post-adaption nonlinear response compression as follows:

$$\begin{aligned} \begin{bmatrix} R' \\ G' \\ B' \end{bmatrix} &= \mathbf{M}_{\text{HPE}} \mathbf{M}_{\text{CAT02}}^{-1} \begin{bmatrix} R_C \\ G_C \\ B_C \end{bmatrix} \\ \mathbf{M}_{\text{HPE}} &= \begin{bmatrix} 0.390 & 0.689 & -0.0787 \\ -0.230 & 1.183 & 0.0464 \\ 0.000 & 0.000 & 0.000 \end{bmatrix} \\ \mathbf{M}_{\text{CAT02}}^{-1} &= \begin{bmatrix} 1.01 & -0.279 & 0.183 \\ 0.454 & 0.474 & 0.0721 \\ -0.00927 & -0.00570 & 1.02 \end{bmatrix}. \end{aligned} \quad (A4)$$

For nonlinear compression, parameters k , F_L , n , N_{bb} which are related to the surrounding environment are calculated using the following formulae:

$$\begin{aligned} k &= 1/(5L_A + 1) \\ F_L &= 0.2k^4(5L_A) + 0.1(1 - k^4)^2(5L_A)^{1/3} \\ n &= Y_b/Y_W \\ N_{bb} = N_{cb} &= 0.7125(1/n)^{0.2}. \end{aligned} \quad (A5)$$

Using these parameters, we express the nonlinear compression as follows,

$$\begin{aligned} R'_a &= \frac{400(F_L R'/100)^{0.42}}{27.13 + (F_L R'/100)^{0.42}} + 0.1 \\ G'_a &= \frac{400(F_L G'/100)^{0.42}}{27.13 + (F_L G'/100)^{0.42}} + 0.1 \\ B'_a &= \frac{400(F_L B'/100)^{0.42}}{27.13 + (F_L B'/100)^{0.42}} + 0.1. \end{aligned} \quad (A6)$$

Preliminary Cartesian coordinates a, b are calculated in order to obtain hue angle h :

$$\begin{aligned} a &= R'_a - 12G'_a - 2B'_a / 11 \\ b &= (1/9)(R'_a + G'_a - 2B'_a) \\ h &= \tan^{-1}(b/a). \end{aligned} \quad (A7)$$

The achromatic response A is defined as follows,

$$A = [2R'_a + (1/20)B'_a - 0.305]N_{bb}. \quad (A8)$$

Using these values, we calculate target lightness J under the illuminant as follows,

$$J = 100(A/A_W)^{c(1.48 + \sqrt{n})}. \quad (A9)$$

A_W is the achromatic response of the illuminant. In this paper we set c to 0.69 corresponding to an average environment. The chroma value C and the colorfulness value M are calculated as follows,

$$\begin{aligned} C &= t^{0.9} \sqrt{J/100} (1.64 - 0.29^n)^{0.73} \\ t &= \frac{(50000/13)N_c N_{cb} e_t (a^2 + b^2)^{1/2}}{R'_Z + G'_Z + (21/20)B'_Z} \\ M &= C F_L^{0.25}. \end{aligned} \quad (A10)$$

The parameters for coefficients values, c_1 , c_2 , K_L are defined as uniform color space values: $c_1 = 0.007$, $c_2 = 0.0228$, $K_L = 1.00$. Color differences by CIECAM02 are defined as follows,

$$\begin{aligned} J' &= \frac{(1 + 100c_1)J}{1 + c_1 J} \\ a_M' &= M' \cos(h) \\ b_M' &= M' \sin(h) \end{aligned} \quad (A11)$$

$$M' = (1/c_2) \ln(1 + c_2 M).$$

Color difference value in the CIECAM02 color appearance model is defined by using lightness value J' and Cartesian coordinates a_M' , b_M' as follows,

$$\Delta E' = ((\Delta J'/K_L)^2 + \Delta a_M'^2 + \Delta b_M'^2)^{1/2}. \quad (A12)$$